In-medium properties of vector mesons: pion cloud effects *

M.D. Cozma
National Institute for Physics and Nuclear Engineering
Atomiştilor 407, 077125 Măgurele-Bucharest, Romania

Dilepton emission in heavy-ion collisions represents a unique possibility for the study of in-medium properties of mesons close to the boundary of chiral symmetry restoration. Emission of dilepton pairs has its main sources in the decay of isoscalar meson π^0 and η and of vector mesons ρ and ω at higher invariant masses, and can be drastically altered in a dense nuclear matter environment, as a consequence of the change of meson properties. We have extended the eVMD model to include πNR and ηNR interactions which has allowed for a study of the influence of the in-medium pion cloud on the properties of the ρ and ω mesons in nuclear matter. Within this model in-medium effects on the η meson are also studied. We present, somewhat off the main topic, a comparison of our dilepton emission model with available experimental data provided by the DLS and HADES collaboration for the heavy-ion reactions C+C and Ca+Ca at 1.04 AGeV and respectively C+C at 2.0 AGeV.

I. INTRODUCTION

Dileptons produced in heavy-ion reactions present an unique opportunity for the study of nuclear matter under extreme conditions, providing a clear view on effective degrees of freedom at high baryon density and temperature. It has been argued that their differential spectra could reveal information about chiral restoration and in-medium properties of hadrons [1–3]. Theoretically, there exists an abundance of models that predict a change of vector meson masses and widths in high density/temperature nuclear matter: Brown-Rho scaling [1] is equivalent with a decrease of vector meson masses in nuclear medium; models based on QCD sum rules [2] and effective hadronic models [4–9] reach similar conclusions.

The resonance model developed by the group in Tübingen and collaborators [10–12] has been employed to describe the properties of the ρ and ω in a high density nuclear matter environment by extracting their in-medium self energies. Contributions due to scattering of vector mesons off nucleons with the excitation of nucleonic resonances aswell as background contributions due to non-resonant scattering or via the exchange of σ mesons have been considered [13]. The model developed so far suffers from a few drawbacks: $\rho\rho\sigma$ and $\omega\omega\sigma$ couplings are poorly known at best and more importantly the present model does not describe, in the limit of very small densities, the vacuum properties of the ρ and ω vector mesons. These two problems can be alleviated by extending the model to include in an effective description all the reaction channels responsible for the vacuum properties of vector mesons and also explicit πNR couplings. This extension is required for the description of the in-medium corrections to the virtual pion cloud which determines the vacuum properties of the ρ and ω mesons.

The first Section of this Report is dedicated to a brief review of the main ingredient of the eVMD model and to its extension by inclusion of explicit πNR and ηNR couplings. We continue in Section III with the exploration of in-medium effects on the properties of pion and eta mesons which are prerequisites for the development of an effect model for the description of ρ and ω mesons in vacuum and the in-medium corrections to those amplitudes in Section IV. We continue with a comparison of the theoretical dilepton spectrum with experimental data provided by the DLS [14, 15] and HADES [16, 17] collaborations. We conclude with a short section dedicated to summary and final remarks.

II. RESONANCE MODEL FOR MESON PRODUCTION

A. The Extended VMD model

In this Section we review those ingredients of the eVMD model [11] of interest for the discussion to follow. The aim of the model is the description of the electromagnetic transition current between a nucleon and a nucleonic resonance

---

* This document represents a progress report for the project "Hadron Properties in Nuclear Matter and Dilepton Emission in Relativistic Heavy-Ion Collisions" (project code: RP9) due on December 15^{th} 2008.

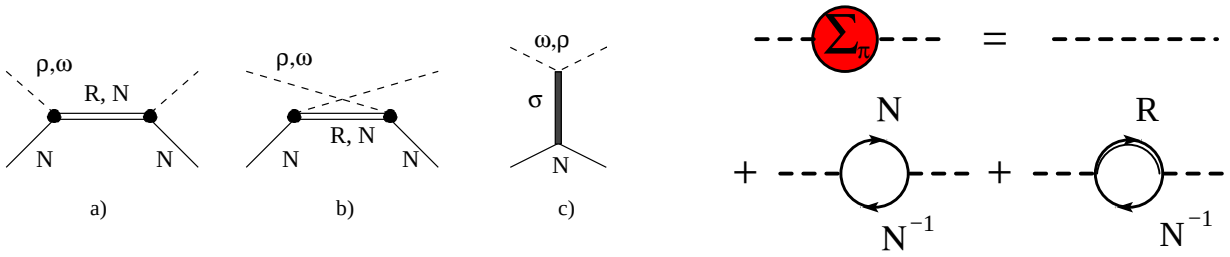

FIG. 1: Left side figure: contribution to vector meson in-medium self-energies considered in [13, 18]: resonance excitation, vector meson Compton scattering off nucleons and sigma meson exchange terms. Right side figure: diagrammatic perturbative expansion of the pion (and eta) self-energy in nuclear matter: nucleon-hole and resonance-hole contributions are added to the vacuum pion (eta) meson propagator.

of spin J. It can be formally written as follows

$$J_\mu(p_R,\lambda_R,p,\lambda) \;=\; e\,\bar{u}_{\beta_1\ldots\beta_2}(p_R,\lambda_R)\,\Gamma^{(\pm)}_{\beta_1\ldots\beta_2\mu}u(p,\lambda), \tag{1}$$

with m_R and m denoting the masses of the nucleonic resonance and nucleon respectively, λ_R and λ are their corresponding helicities and the upper index $\pm$ denotes a resonance of normal and abnormal parity respectively. Making use of Lorentz covariance, the vertex operator $\Gamma^{(\pm)}_{\beta_1\ldots\beta_2\mu}$ can be written, in its most general form, as

$$\begin{aligned}\Gamma^{(\pm)}_{\beta_1\ldots\beta_2\mu} &= q_{\beta_1}\cdots q_{\beta_{l-1}}\,\Gamma^{(\pm)}_{\beta_l\,\mu}\\ \Gamma^{(\pm)}_{\beta,\mu} &= \sum_k \Gamma^{(\pm)\,k}_{\beta\,\mu}\,F^{(\pm)}_k\,.\end{aligned} \tag{2}$$

Here, q denotes the momentum of the emitted (or absorbed) photon. The Dirac structure of the interaction vertexes is fully absorbed in the matrices $\Gamma^{(\pm)\,k}_{\beta\mu}$, while the scalar functions $F^{(\pm)}_k$, called covariant form-factors, contain the dynamics. In the case of the eVMD only the operators $\Gamma^{(\pm)\,k}_{\beta\mu}$ which give a non-zero contribution on-shell are considered, which reduces their number at 2 (for spin 1/2 resonances) and 3 (for spin 3/2 and higher resonances). Their actual expressions can be found in [11].

In the vector meson dominance model the coupling of photons to hadrons, and in particular to the nucleon-resonance system, is supposed to take place via the exchange of a intermediate vector meson in the original version and a vector meson and its excited states in the extended one, which implies the following form for the electromagnetic current: $J_\mu = -e\sum_V \frac{m_V^2}{g_V}V_\mu$, where V_μ denotes the vector meson field operator and the factor in front of it is a consequence of electric charge universality. With this assumption it is not difficult to see that the covariant form factors can be put in the form

$$F^{(\pm)}_k(q^2) \;=\; \sum_V \frac{f^{(\pm)}_{VNR,k}}{g_V}\,\frac{1}{1-q^2/m_V^2}. \tag{3}$$

The asymptotic form of the covariant form-factors is fixed using quark-model arguments (known as quark-counting rules, see [19]) fixing not only the minimum number of intermediate vector mesons needed, but also reducing the number of free parameters (meson-nucleon-resonance couplings). Consequently, the expressions for the form-factors can be written as

$$F^{(\pm)}_1(q^2) = \frac{\sum_{j=0}^{n+1} C^{(\pm)}_{1j}\,q^{2j}}{\prod_{i=1}^{l+3+n}(1-q^2/m_i^2)}\,, \qquad F^{(\pm)}_{2,3}(q^2) = \frac{\sum_{j=0}^{n} C^{(\pm)}_{2,3j}\,M^{2j}}{\prod_{i=1}^{l+3+n}(1-q^2/m_i^2)}, \tag{4}$$

with $l+3+n$ the number of vector mesons ($l+1/2$ being the spin of the resonance under consideration). This expression is equivalent with Eq. (3) in the no-width approximation. Finally, the couplings $C_{1,2,3j}$ are fitted to the "experimental" values for the helicity amplitudes $A_{3/2}$, $A_{1/2}$ and $S_{1/2}$ which can be defined by suitable labeling the contraction of Eq. (1) with the photon polarization four-vector.

Resonance	Parity	Spectroscopic Notation	Γ_{total}	Γ_π	$g_{\pi NR}$	Γ_η	$g_{\eta NR}$
N(938)	+		0.0	0.0	13.60	0.0	3.27
N(1535)	-	S11	0.150	0.100	0.98	0.075	2.08
N(1650)	-	S11	0.150	0.120	0.86	0.007	0.48
N(1520)	-	D13	0.120	0.066	3.02	-	-
N(1700)	-	D13	0.100	0.010	0.58	0.005	2.04
N(1440)	+	P11	0.350	0.220	2.75	-	-
N(1710)	+	P11	0.100	0.015	0.40	0.020	1.31
N(1720)	+	P13	0.150	0.020	0.55	-	-
N(1900)	+	P13	0.500	0.130	0.92	-	-
Δ(1620)	-	S31	0.150	0.040	0.85	-	-
Δ(1900)	-	S31	0.200	0.040	0.80	-	-
Δ(1700)	-	D33	0.300	0.045	2.12	-	-
Δ(1940)	-	D33	0.500	0.100	1.53	-	-
Δ(1750)	+	P31	0.300	0.030	0.90	-	-
Δ(1910)	+	P31	0.250	0.060	1.03	-	-
Δ(1232)	+	P33	0.120	0.120	12.26	-	-
Δ(1600)	+	P33	0.350	0.070	2.22	-	-
Δ(1920)	+	P33	0.200	0.030	0.74	-	-

TABLE I: List of the nucleonic resonances included in the resonance model used to describe in-medium properties of pi and eta mesons, together with their total decay widths, partial decay widths into the channels $R \to N\pi$ and $R \to N\eta$ and the corresponding values for the coupling constants.

B. Pion-nucleon-resonance couplings

The eVMD model presented in the previous Section contains explicit couplings of the ρ and ω mesons to nucleon resonances and manages to describe, among other observables, the partial decay widths of the included resonances into vector mesons. As can be seen from Table I most of resonances of spin 1/2 and spin 3/2 have a large fraction of their totaldecay widths contributing to the decay channel $R \to N\pi$ (a complete list of all resonances included in the eVMD model and their decay channels can be found in [20]). It is therefore mandatory, in order to obtain a unified description of meson-nucleon-resonance interactions to extend the model by providing explicit couplings of the pi meson to these resonances. The first step towards the construction of such a model is represented by a choice of the interaction Lagrangian. In this respect it is worth mentioning the results of Ref. [21] in which it is shown how to construct consistent interaction terms for higher spin particles with an explicit example for the spin 3/2 Δ isobar. The method relies on building gauge invariant interactions, with gauge symmetry broken just by the mass term, thus ensuring that only fields with maximal spin (3/2 for a Δ isobar) are propagated in the intermediate states. At the same time invariance guarantees that scattering amplitudes are finite in the t channel.

Following the results of [21] we have constructed the following interaction terms for the resonances of spin 1/2 and 3/2 included in this study

$$\mathcal{L}^{(S11/S31)} = -g\overline{\psi}_R\,\gamma_5\,\gamma_\mu\,\vec{\tau}\,\psi\,\partial^\mu\,\vec{\pi} + h.c. \tag{5}$$

$$\mathcal{L}^{(P11/P31)} = -g\overline{\psi}_R\,\gamma_5\,\gamma_\mu\,\vec{\tau}\,\psi\,\partial^\mu\,\vec{\pi} + h.c. \tag{6}$$

$$\mathcal{L}^{(P31/P33)} = -g\overline{\psi}\,\gamma_5\,\gamma_\mu\,\vec{\tau}\,\widetilde{G}^{\mu\nu}\,\partial_\nu\,\vec{\pi} + h.c. \tag{7}$$

$$\mathcal{L}^{(D31/D33)} = -g\overline{\psi}\,\gamma_5\,\gamma_\mu\,\gamma_\nu\,\vec{\tau}\,G^{\mu\rho}\,\partial_\rho\partial^\nu\,\vec{\pi} + h.c. \tag{8}$$

$$\widetilde{G}^{\mu\nu} = \frac{1}{2}\varepsilon^{\mu\nu\rho\sigma}\,G_{\rho\sigma}; \qquad G^{\mu\nu} = \partial^\mu\,\psi^\nu - \partial^\nu\,\psi^\mu$$

where the upper index of each Lagrangian term specifies to what type of resonance (in spectroscopic notation) it can be applied to. The field ψ denotes a nucleon field, while the isospin transition operator $\vec{\tau}$ applies to isospin 1/2 resonances, for the description of isospin 3/2 resonances one has to replace it with the isospin $1/2 \to 3/2$ transition operator $\vec{T}^\alpha$. The list of all resonances included in the present study is presented in Table I where also the values of the corresponding coupling constants $g_{\pi NR}$ are shown. They were extracted by requiring that the partial decay width $\Gamma_{R\to\pi N}$ is reproduced on-shell. Eventhough this represents a minimal procedure the resulting values for the coupling

constants are in qualitative agreement with the ones extracted be employing more sophisticated model, as the ones in Ref. [22–24]. To cut off the wrong behavior of pointlike interactions at small distances at dipole form factor with the cut-off value Λ=1.0 GeV is included at each πNR vertex. For the background scattering of pions off nucleons the customary pseudovector coupling is used with a value of the coupling constant as listed in Table I. It is desirable that the current model parameter space is constrained by a fit to a larger experimental database, as for example meson production total and differential cross-sections. Work in this direction is planned for the near future.

C. Eta meson production model

As can be seen from Table I there a few resonances which have non-vanishing partial decay widths into the η meson, of which N(1535) is the most proeminent one. In terms of quantum numbers the only difference between the pion and eta is isospin. As a consequence, for the description of ηNR vertices, the same interaction terms as used in the previous Section can be used. The excitation of nucleonic resonances has to be supplemented by a term describing the non-resonant scattering of η mesons of nucleons. The alternatives for such a term are a pseudoscalar or an pseudovector coupling. Unlike for the case of pions, constraints on theoretical models for the nucleon-nucleon interaction or eta meson-photo production on nuclei have not been able to favor one or the other. Moreover even when a definite choice is made, fits to experimental data yield values of the $NN\eta$ coupling constant over a large range. For this work we have chosen the following interaction Lagrangian

$$\mathcal{L}_{NN\eta} \;=\; -g_{NN\eta}\,\overline{\psi}\,\gamma_5\,\gamma_\mu\,\psi\,\partial^\mu\,\eta, \tag{9}$$

and have taken for the coupling constant a value $g_{NN\eta} = 3.27$, extracted from a fit of the one-boson exchange (OBE) model for NN interaction of Fleischer and Tjon to elastic nucleon-nucleon scattering data. It is worth mentioning that another model belonging to this category, the Bonn CD OBE model finds a value of the coupling constant consistent with zero.

III. IN-MEDIUM PROPERTIES OF PI AND ETA MESONS

This Section is devoted to the presentation of the in-medium properties of the π and η mesons, making use of the model briefly presented in II. Since both meson are scalar particles the self-energy is a scalar and can be determined by solving a Dyson-Schwinger equation. In the right-hand side plot of Figure 1 the diagrammatic solution of such an equation is presented: the in-medium self-energy receives, to leading order in perturbation in density, contributions from the excitation of nucleon-hole and resonance-hole pairs. Finally the spectral function can be extracted

$$A_{\pi/\eta}(k^2,|\vec{k}|) \;=\; \frac{1}{\pi}\,\frac{Im\,\Sigma_{\pi/\eta}(k^2,|\vec{k}|)}{[k^2-m_0^2+Re\,\Sigma_{\pi/\eta}(k^2,|\vec{k}|)]^2+[Im\,\Sigma_{\pi/\eta}(k^2,|\vec{k}|)]^2} \tag{10}$$

A. In-medium effects on pions

We will start this subsection with a brief review of the so called "three-level model" used to describe in-medium properties of pions in [25]. In this model only terms due to the excitation of nucleon-hole and $\Delta(1232)$-hole pairs have been included in the expression for the self-energy, as they contribute the most at low energies. Furthermore, one works in a non-relativistic and low density approximation. As a consequence the expressions for the nucleon-hole and delta-hole contributions to in-medium pion self-energy can be written in a closed form, leading to a in-medium pion propagator with the following structure [25]

$$G_\pi(k) \;=\; \frac{S_1(\vec{k})}{k_0^2-\omega_1^2(\vec{k})}+\frac{S_2(\vec{k})}{k_0^2-\omega_2^2(\vec{k})}+\frac{S_3(\vec{k})}{k_0^2-\omega_3^2(\vec{k})}, \tag{11}$$

where ω_1, ω_2 and ω_3 represent the dispersion relations of three-quasiparticles belonging to the so-called nucleon-hole branch, pion branch and delta-hole branch respectively. At small densities and momenta the pion branch is dominant (S_2=1) while when these two variables are increased the pion becomes an admixture of mainly delta-hole and nucleon-hole pairs. This pattern is of course exhibited also in a fully relativistic model at arbitrary density with the exception that the various branches are not as clearly separated as in this very simple model.

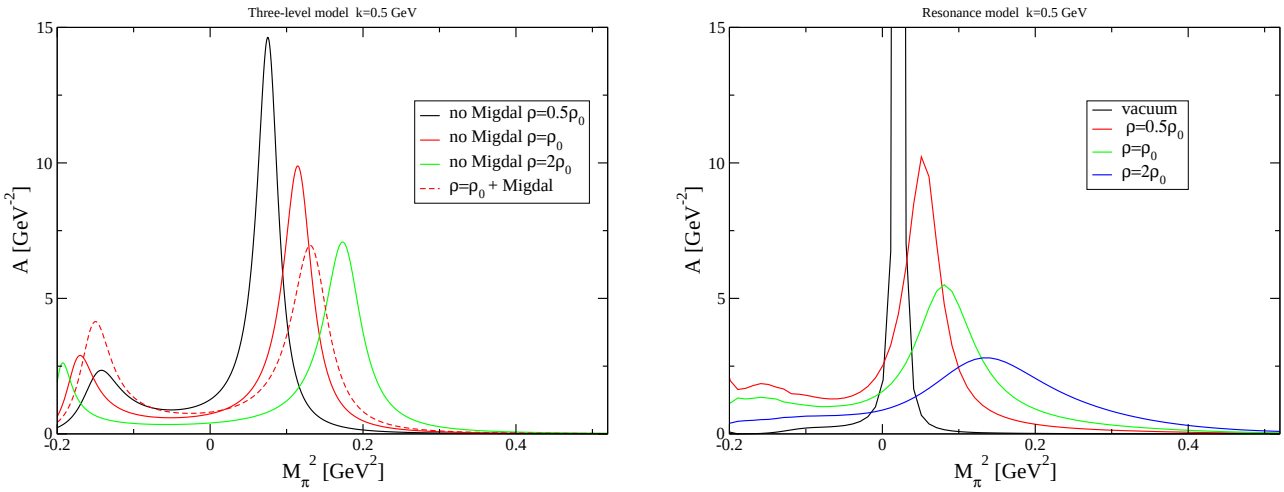

FIG. 2: In-medium pion spectral function computed within the three-level model (left side plot) and in the resonance model (right side plot) at pion three momentum $|\vec{k}|$ =0.5 GeV and various values for density.

In the following we will compare the in-medium spectral function of the pi meson at various densities as extracted from the "three-level" model with the ones obtained by employing the resonance model of last section. Results are presented in Figure 2, the left-hand side plot corresponding to the tree-level model, while the right hand side to the fully relativistic resonance model. In the case of the "three-level" model we have chosen the $NN\pi$ and $\Delta N\pi$ coupling constants to match the ones used in the resonance model. In this case it is clearly seen the increase, with density, of the pole mass and decay width of the pion branch, while a proeminent delta-hole branch develops at negative invariant masses. Including short range repulsion interactions terms, known as Migdal interaction terms, between nucleon and Δ resonances leads to a further, though moderate, shift of the original pion branch.

Turning to the resonance model results, we observe that they are qualitatively similar. We observe in this case too, an upward shift of the pion branch mass with increasing density. Broadening effects on the pion branch are more pronounced than in the 3-level model case, resulting in an almost disappearance of the quasiparticle properties at densities $\rho \geq 2\rho_0$. An invariant negative masses the delta-hole peak observed within the three-level model transforms into an almost uniform background which results from a superposition of the contributions from the various nucleonic resonances included. Our results are qualitatively similar to other works. Within coupled-channel approach to meson nucleon scattering the authors of Ref. [8, 26] find out that the in-medium pion spectral function has a complicated invariant mass dependence structure due to channel coupling effects, their results also indicating that at high densities the quasiparticle properties of the pion are essentially lost.

B. In-medium properties of the eta meson

Results for the in-medium η meson spectral functions are presented in Figure 3 for two value of its three-momentum: $|\vec{k}|$=0.0 GeV and $|\vec{k}|$=0.5 GeV. At very low momenta, as can be seen from Equation 5, only S wave contributions to the in-medium self energy survive. As a result curves in the left-hand side plot of Figure 3 are a measure of the N(1535) resonance, and to a much lesser extent of N(1650), influence on in-medium properties of eta. As in the case of vector mesons [18], the excitation of a proeminent resonance leads to the appearance o secondary peak, here at invariant masses of 650 MeV. The original η branch suffers a downward mass shift with increasing density , accompanied by an important increase of the decay widths:$\Gamma_{coll} = 50MeV$ at $\rho = 2\rho_0$. The situation changes qualitatively at finite three-momentum due to the interference of the resonance and background contributions: the pole mass of the η meson shifts slightly upwards with increasing density, while the in-medium scattering off nucleons results in a sizable decay widths at invariant masses below the pole mass.

In Ref. [27] the in-medium properties of the η meson have been determined within a chiral unitary approach which solves a coupled channel Bethe-Salpeter equation to obtain an effective ηN interaction in the medium, which generates the coupling of the N(1535) in a dynamical way. The resulting spectral function for the η meson is qualitatively the same with ours at zero three-momentum. Due to the fact that the strength of the dynamically generated ηNR is weaker than our, the authors find that in nuclear matter the effective η mass scales like $m^*_\eta/m_\eta \simeq$1-0.05ρ/ρ_0 together with a rather weak collisional broadening. The authors of [28] find within a quark-meson coupling model a downward

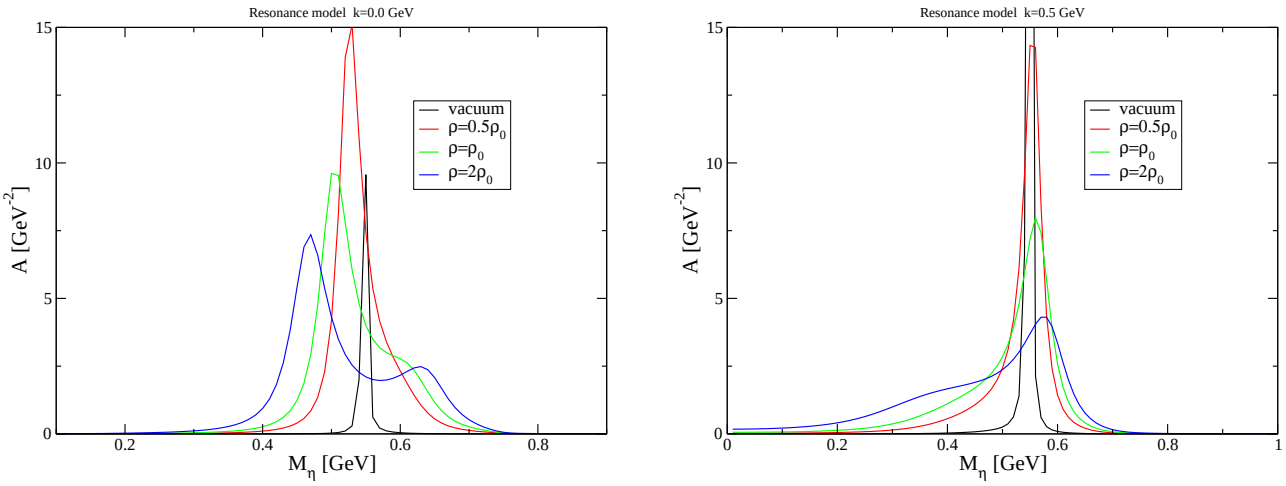

FIG. 3: In-medium eta spectral functions computed within the resonance model for to values of the modulus of the eta's three-momentum: k=0.0 GeV (left-side plot) and k=0.5 GeV (right-side plot).

mass-shift which is in magnitude comparable with ours.

It is well known that one of the important sources for dilepton emission in heavy-ion collisionin in the low to intermediate invariant mass range is the Dalitz decay of the η meson into a dilepton pair and a photon. In a comparison of dilepton emission spectra in C+C collisions at 2.0 AGeV [13, 29] with experimental data obtained by the HADES collaboration it was revealed that theoretical models fail to properly reproduce experimental data in the mass region 0.2-0.6 GeV, a few solutions, not involving in-medium properties of the η meson, being put forward [29]. It would be interesting to address the question wether dilepton emission spectrum in heavy-ion collisions is at all affected by changes in the in-medium properties of the η meson.

IV. PION CLOUD CORRECTIONS TO VECTOR MESONS

This Section is devoted to the description of the last ingredient of our unified model for meson-nucleon-resonance interaction in both vacuum and nuclear matter. We have discussed so far the part of the Lagrangian that describes the interaction of mesons with nucleons and nucleonic resonances both in vacuum and matter. Consistency requires that when the low density limit is approached in the in-medium calculations one should recover vector meson spectral functions that are consistent with the known properties of these particles in vacuum. For that purpose we need to add a term to the interaction that takes into account all major decay channel in vacuum for both ρ and ω mesons.

A. Effective model in vacuum

The model used here for the description of the ρ mesons in vacuum mirrors the one presented in Ref. [25]. We will only present its essential details here. In vacuum, the ρ meson has a decay width Γ_ρ=150.0 MeV, the decay into a two-pion final state having a branching ratio close to 100%. To construct an interaction for these decay channel one starts from the free Lagrangian for pions and ρ mesons and introduces an interaction via minimal substitution

$$\mathcal{L}_0 = \frac{1}{2}\partial_\mu \vec{\pi}\cdot\partial^\mu\vec{\pi} - \frac{1}{2}m_\pi^2\,\vec{\pi}\cdot\vec{\pi} - \frac{1}{4}\rho_{\mu\nu}\rho^{\mu\nu} + \frac{1}{2}m_\rho^2\,\rho_\mu\,\rho^\mu \tag{12}$$

$$\mathcal{L}_{\pi\rho} = \frac{i}{2}g\,\rho_\mu^a\,(\partial^\mu\,\pi_i\,T_{ij}^a\,\pi_j + \pi_i\,T_{ij}^a\,\partial^\mu\,\pi_j) - \frac{1}{2}g^2\,\rho_\mu^a\,\rho^{\mu,b}\,T_{ij}^a\,\pi_j,\,T_{ik}^b\,\pi_k \tag{13}$$

where latin subscripts refer to the isospin degree of freedom. The process of minimal substitution leads to the appearance to both $\rho\pi\pi$ and $\rho\rho\pi\pi$ vertices. To fix the bare parameters present in the above Lagrangian, one demands that vacuum ρ meson properties like mass and decay widths are reproduced. This is equivalent with the description of the pion electromagnetic form-factor (assuming vector meson dominance). For that one needs to compute corrections

to ρ meson propagator at least to first order in perturbation theory. Those expressions read

$$i\Sigma_{\mu\nu}(q)^{(\rho)} \;=\; g^2 \int \frac{d^4k}{(2\pi)^4} \frac{(2k+q)_\mu\,(2k+q)_\nu}{[(k+q)^2-m_\pi^2+i\varepsilon]\,[k^2-m_\pi^2+i\varepsilon]} - 2g^2\,g_{\mu\nu} \int \frac{d^4k}{(2\pi)^4}\,\frac{1}{k^2-m_\pi^2\,i\varepsilon}\,, \tag{14}$$

corresponding to the two leftmost Feynman diagrams in Figure 4. In vacuum, for the loop integrals of these type, known as two-point functions, one can arrive at analytical expressions within the scheme of dimensional regularization. As this will not be the case when in-medium effects are introduced, we prefer to regularize them by employing the Pauli-Villars scheme, which loosely explained consists in the introduction of heavy mass intermediate propagators which ensure convergence of the integrals under consideration. In this case it can be formally written as [25]

$$\Sigma_{\mu\nu}(q,m_\pi) \;\longrightarrow\; \Sigma_{\mu\nu}(q,m_\pi) + \sum_{i=1}^{3} c_i\,\Sigma_{\mu\nu}(q,M_i) \tag{15}$$

with the value of the masses conveniently chosen and coefficients c_i fixed by requiring cancellation of monomials of powers higher than 1 in k^2. For the present case we have made the following choice: $c_1 = -3$, $c_2 = 3$ $c_3 = -1$, $M_i^2 = m_\pi^2 + i\,\Lambda^2$ and Λ =1.0 GeV.

The situation of the ω vector meson is technically more involved. There are three major channels contributing to a total decay width of Γ_ω=8.4 MeV with the following branching ratios: $B_{\omega\to 3\pi}$=88.8%, $B_{\omega\to\pi^0\gamma}$=8.5% and $B_{\omega\to\pi^+\pi^-}$=2.2%. For the description of the first decay we use the effective model of Gell-Mann-Sharp-Wagener [30] which assumes that the decay into 3 pions is a two-step process: first a decay into a $\rho\pi$ pair occurs followed by the decay of the ρ vector meson into two pions. For the other two interaction terms commonly used in the literature have been used [22]

$$\mathcal{L}_{\omega\rho\pi} \;=\; -\frac{g_{\omega\rho\pi}}{4m_\pi}\,\vec{\pi}\epsilon_{\mu\nu\alpha\beta}\vec{\rho}^{\mu\nu}\omega^{\alpha\beta}\,, \tag{16}$$

$$\mathcal{L}_{\omega\pi\gamma} \;=\; -e\frac{g_{\omega\pi\gamma}}{4m_\pi}\,\pi_0\,\epsilon_{\mu\nu\alpha\beta}\,\omega^{\mu\nu}F^{\alpha\beta}\,, \tag{17}$$

$$\mathcal{L}_{\omega\pi\pi} \;=\; -\frac{g_{\omega\pi\pi}}{2m_\pi}\,\omega_\mu\,(\partial^\mu\vec{\pi}\cdot\vec{\pi}+\vec{\pi}\cdot\partial^\mu\vec{\pi})\,. \tag{18}$$

As in the case of the ρ meson the bare parameters of the interaction Lagrangian are fixed by requiring the description of vacuum ω meson properties. The expressions of the contributions to the vacuum self-energy (see Figure 4) read

$$i\Sigma^{(\omega\rho\pi)}_{\beta_1\beta 2}(q,m_\pi,m_\rho) \;=\; \frac{g^2_{\omega\rho\pi}}{4m_\pi^2}\int\frac{d^4\,k}{(2\pi)^4}\,\varepsilon_{\mu_1\nu_1\alpha_1\beta_1}\varepsilon_{\mu_2\nu_2\alpha_2\beta_2}\,q^{\alpha_1}q^{\alpha_2}\,(k+q)^{\mu_1}(k+q)^{\mu_2}D_F^{\nu_1\nu_2}(k+p)\,S_F(k) \tag{19}$$

$$i\Sigma^{(\omega\pi\pi)}_{\beta_1\beta_2}(q,m_\pi) \;=\; \frac{g^2_{\omega\pi\pi}}{m_\pi^2}\int\frac{d^4k}{(2\pi)^4}\,(2k+q)_{\beta_1}\,(2k+q)_{\beta_2}\,S_F(k)\,S_F(k+q) \tag{20}$$

$$D_F^{\mu\nu}(p) \;=\; \frac{-g^{\mu\nu}+p^\mu p^\nu/p^2}{p^2-m_v^2+i\,\Sigma_0(p^2)} \qquad\qquad S_F(p)=\frac{1}{p^2-m_\pi^2+i\varepsilon}$$

the contribution for the $\omega\to\pi\gamma$ having the same expression as the one for the decay $\omega\to\rho\pi$ except an isospin factor and the replacement of the ρ vacuum propagator with the one for a massless spin 1 particle. As in case of the ρ meson the self-energy amplitudes are regularized via the Pauli-Villars scheme, Eq. 15 leading to the extraction of the three coupling constants and the bare ω meson mass. Knowing the self-energy tensor $\Sigma_\mu\nu$ the expression of the scalar projection that enters in the expression for the spectral function similar to Eq. 10 is easily obtained by a contraction with the 4-dimensional transverse projection operator $\Sigma_0(q) = \frac{1}{3}\,P^T_{\mu\nu}\,\Sigma^{\mu\nu} = (g^{\mu\nu}-q^\mu q^\nu/q^2)\,\Sigma^{\mu\nu}$.

B. Medium corrections to the rho and omega mesons

In the previous Subsection we have presented an effective model which allows for a full description of the ρ and ω vector meson properties in vacuum. The transition to the in-medium case is obtained by recalling that our model includes interaction terms due to pion and vector meson scattering off nucleons with or without excitation of resonances. Due to the interactions of the virtual pions and ρ mesons in the pion cloud with the nucleons from nuclear matter the vacuum pion/rho propagators are replaced by the in-medium ones. We have discussed the in-medium pion propagator in Section II B while the in-medium ρ propagator has been discussed elsewhere [13, 18]. In the following we will briefly describe the medium correction to the interaction vertices. A diagrammatic representations of the

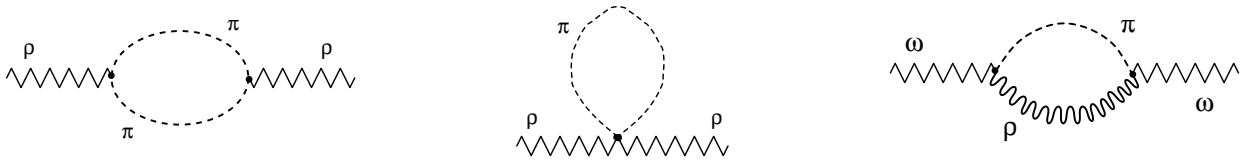

FIG. 4: Feynman diagrams contributing to the vacuum self-energy of the rho meson: decay into two pions (a)) and pion tadpole contribution (b)). There are three diagrams contributing to omega meson vacuum self-energy of which the one corresponding to the leading decay channel $\omega \to \rho\pi$ is depicted in subfigure c). The decay channel $\omega \to \gamma\pi$ is depicted by a similar diagram with the ρ propagator replaced by a photon propagator, while for the reaction $\omega \to \pi\pi$ one has to substitute initial and final ρ states in diagram a) with ω vector mesons.

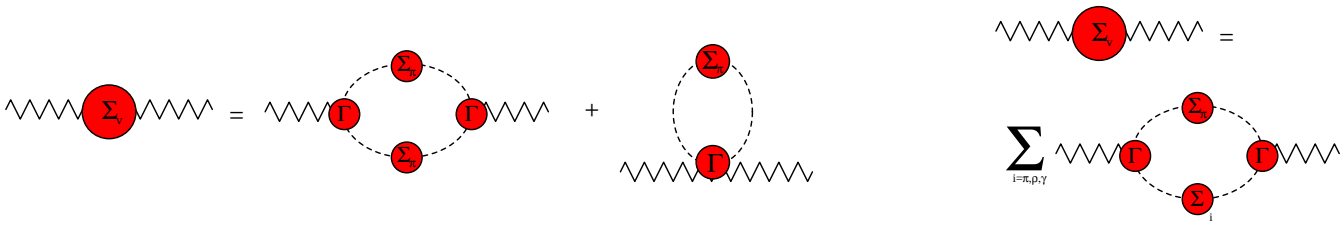

FIG. 5: Diagrammatic representation for the integral equations of the in-medium self-energies of the ρ (left) and ω (right) mesons.

in-medium corrections to the pion cloud and vertices are presented in Fig. 5, in which the terms corresponding to the first order expansion in density of the in-medium rho (left-side picture) and omega (right-side picture) propagators are presented.

To be more specific we present the analytical expressions that have to be evaluated in order to extracted the in-medium rho meson self-energy

$$i\Sigma^{ij}_{\mu\nu(q)} = \frac{1}{2}\int \frac{d^4k}{(2\pi)^4}\, iD_\pi(k)\,\Gamma^i_{\mu ab}(k,q)\, iD_\pi(k+q)\,\Gamma^j_{\nu ba}(k+q,-q) \tag{21}$$

$$+\frac{1}{2}\int \frac{d^4k}{(2\pi)^4}\, iD_\pi(k)\,\Gamma_{\mu\nu aa}(k,k,q) \tag{22}$$

$$\Gamma^i_{\mu ab}(k,q) = g\varepsilon_{iab}\,(2k+q)_\mu + \tilde{\Gamma}^i_{\mu ab}(k,q) \tag{23}$$

$$\Gamma^{ij}_{\mu\nu ab}(k_1,k_2,q) = 2ig^2\,(\delta_{ab}-\delta_{ia}\delta_{jb})\delta_{ij}\,g_{\mu\nu} + \tilde{\Gamma}^{ij}_{\mu\nu ab}(k_1,k_2,q)\,. \tag{24}$$

The vertex operators and pion propagators are fully in-medium quantities and as is explicitly shown above the in-medium vertices are the sum of the bare ones and in-medium corrections. In-medium corrections to $\rho\pi\pi$ and $\rho\rho\pi\pi$ are generated at a first order in an expansion in density by coupling all external legs of the vacuum vertex Feynman diagrams to nucleon-hole or nucleon-resonance loops. In Figure 6 a small sample of the possible corrections to $\rho\pi\pi$ (left) and $\rho\rho\pi\pi$ (right) vertices are shown. Interactions of ρ and ω mesons with the in-medium nucleons are governed by the well known terms used in the construction of OBE models

$$\mathcal{L}_{NN\rho} = g^V_\rho\,\overline{\psi}\gamma^\mu\,\vec{\tau}\,\psi\cdot\vec{\rho}_\mu + \frac{ig^T_\rho}{4m_N}\,\overline{\psi}\,\sigma^{\mu\nu}\,\vec{\tau}\,\psi\cdot(\partial_\mu\vec{\rho}_\nu - \partial_\nu\vec{\rho}_\mu)\,, \tag{25}$$

$$\mathcal{L}_{NN\omega} = g^V_\omega\,\overline{\psi}\gamma^\mu\psi\omega_\mu\,, \tag{26}$$

the values of the coupling constants reproducing the ones used in the Bonn OBE model for the NN interaction: ${g^V_\rho}^2/4\pi$=0.84, g^T_ρ/g^V_ρ=6.09 and ${g^V_\omega}^2/4\pi$=20.00. Couplings of the type ρNR and ωNR are described by employing the eVMD model and finally the πNR interaction making use of the model developed in Section II B. In general one arrives at lengthy expressions involving traces Dirac matrices which are conveniently evaluated with the use of the symbolic programming utility FORM. As an example we present the relatively simple expression for the $\rho\pi\pi$ vertex

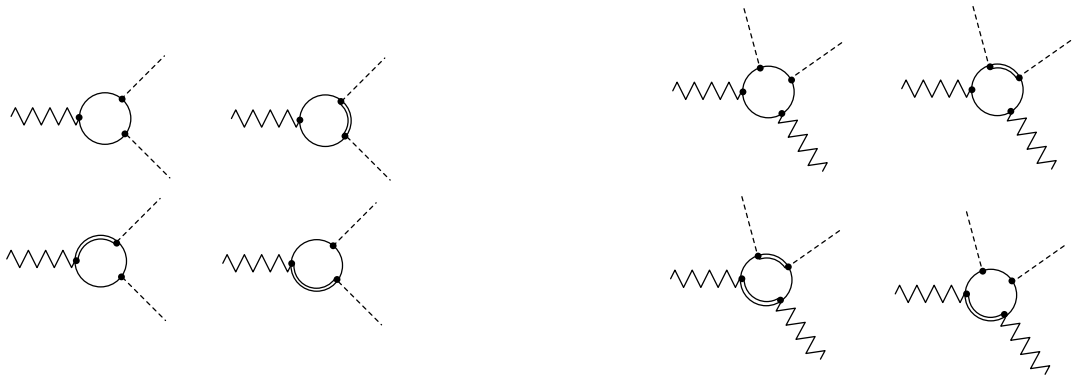

FIG. 6: In-medium contributions to the $\rho\pi\pi$ (left) and $\rho\rho\pi\pi$ (right) vertices. Dashed lines, wavy lines, full lines and double lines represent respectively pions, rho mesons, nucleons and nucleonic resonances. To obtain the contributions due to the presence of the nuclear medium for the $\omega\rho\pi$ vertex one has to replace one of the external pions with an omega meson.

correction obtained by coupling the rho meson and the virtual pions to a nucleon-hole loop

$$\tilde{\Gamma}^i_{\mu ab}(k,q) = \int_{|\vec{p}|<p_F} \frac{d^3\vec{p}}{(2\pi)^3}\,\mathrm{Trace}\Big\{\big[g_\rho^V\,\gamma_\mu + \frac{g_\rho^T}{2\,m_N}\,\sigma_{\mu\nu}q^\nu\big]\,\frac{\not p+\not q+m_N}{(p+q)^2-m_N^2+i\varepsilon}\,\theta(|\vec q+\vec p|-p_F)\,\gamma_5\not k \\ \frac{\not p+\not q+\not k+m_N}{(p+q+k)^2-m_N^2+i\varepsilon}\,\theta(|\vec q+\vec p+\vec k|-p_F)\,\gamma_5\,(\not k+\not q)\,\frac{\not p+m_N}{2m_N}\Big\}\,\mathrm{Trace}\{\tau_i\,\tau_a\,\tau_b\}. \quad (27)$$

From a formal point of view the evaluation of medium effects on ω meson proceeds in a very similar way, but one has now to consider vertex corrections to the $\omega\rho\pi$, $\omega\pi\gamma$ and $\omega\pi\pi$ vertices. In the evaluation of the second the eVMD photon-nucleon-resonance couplings are used. For the results presented in this report not all possible vertex corrections contributing to the first order density corrections to vertices have been computed, but only those coupling to nucleon-hole in-medium loop and some of the delta-hole contributions. Work is in progress to account for all significant contributions involving nucleon resonances of spin 1/2 and 3/2 present in the eVMD model.

In the following we present results for the in-medium spectral functions of the ρ and ω vector mesons using the model discussed in this section, averaged over the transversal and longitudinal directions. To obtain the results depicted in Fig. 7 only contributions due to medium corrections to the virtual pion cloud and to meson vertices have been considered. Contributions due to direct scattering of vector mesons off the nucleons in the nuclear medium (see Fig. 1) have been omitted. In the left-side plot of Fig. 7 the spectral function of the ρ meson at various densities is shown. In the right-side plot of the same figure results of a similar calculation for the ω meson are presented. As a common feature an increase of the vector meson mass with increasing density, more pronounced for the ω meson, but preserving the quasiparticle properties of either meson is observed. A feature, which at a first look seems rather disturbing is the decrease of the ρ meson decay widths with increasing density. Such a result is counter-intuitive as one would expect the opposite since by increasing density a larger part of the phase-space becomes available and the imaginary part of the self-energy, which determines the value of the decay widths and is related through unitary to decay probabilities, should therefore increase. This issue is currently under investigation.

V. DILEPTON EMISSION SPECTRUM: COMPARISON WITH EXPERIMENTAL DATA

In a previous Report [18] the in-medium spectral functions of the ρ and ω vector mesons have been calculated. Contributions from scattering of mesons off the nucleons in nuclear matter with the excitation of nucleonic resonances, as well as background terms due to non-resonant scattering have been considered. Predictions for the theoretical dilepton spectrum, by employing several scenarios for in-medium modification of vector mesons have been provided [18]. In this Section we would like to present a first comparison between the theoretical predictions and experimental data obtained by the DLS (BEVALAC) [14, 15] and HADES(GSI) [16, 17] collaborations. Available experimental filters have allowed a comparison with the following experimental data sets: C+C and Ca+Ca at 1.04 AGeV incident beam energy for the DLS collaboration data and C+C at 2.0 AGeV for the HADES experimental data.

In Fig. 8 a comparison between theoretically predicted spectra and the experimentally measured ones, for the mentioned reactions are presented. For each case theoretical spectra involving four medium effects scenarios have been simulated. Curves labelled "vacuum" correspond to simulations in which no in-medium effects on vector mesons

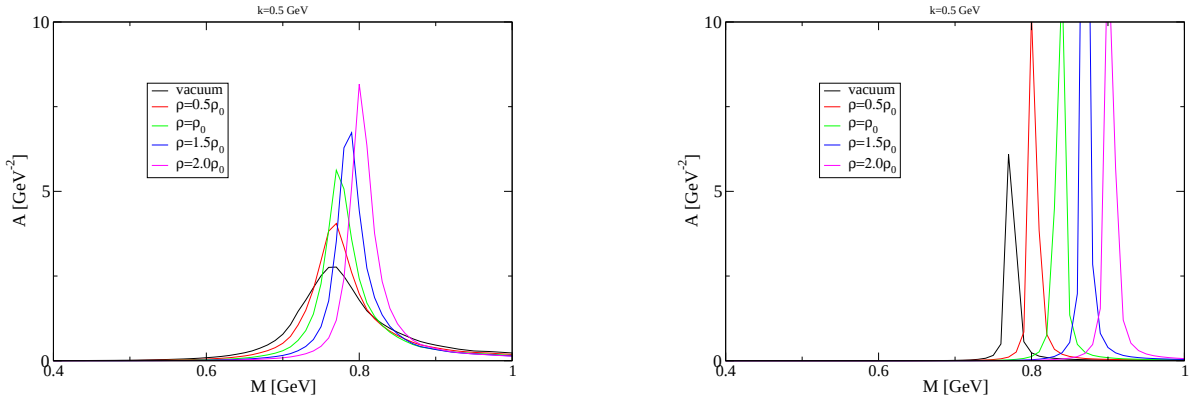

FIG. 7: In-medium rho (left) and omega (right) meson spectral functions obtained by considering medium contribution to the virtual pion cloud and vertex corrections to the vacuum self-energy diagrams.

have been considered. This corresponds to the situation when due to the small vacuum decay widths of the ω meson a sharp peak at its pole mass should appear in the dilepton spectrum. In real world experimental data this should lead to a pronounced peak at invariant dilepton masses close to 0.8 GeV. Such an effect is not observed in any of the cases presented here and an absence of medium effects on vector meson properties is therefore excluded by experimental data.

A second scenario entails a downward shift with increasing density of vector meson masses known as Brown-Rho scaling, formally described by $m_V^* = m_V(1 - \alpha\rho/\rho_0)$ with ρ the local baryon density and $\alpha = 0.2$. This scenario has been supplemented by a linear density dependent collisional width $\Gamma_V^{\rm tot} = \Gamma_V^{\rm vac} + \rho/\rho_0\Gamma_V^{\rm coll}$, with $\Gamma_\omega^{\rm tot}$=125 MeV, $\Gamma_\rho^{\rm tot}$=250 MeV at $\rho = \rho_0$. Results for this scenario are labeled "br+cb" in Figure 8. For all reactions presented here this scenario fails to reproduce experimental data in the intermediate invariant mass region. Results become worse with the increasing of the atomic weight of the collided nuclei, cases in which medium effect are expected to be more pronounced.

The last two scenarios take into account modifications of vector meson properties inside nuclear matter as extracted by employing the eVMD model to compute their in-medium spectral functions. Calculations "spf resonances" and "spf all" include contributions to the in-medium vector meson self-energies only due to excitation of nucleonic resonances and respectively nucleonic resonances and background terms. Differences with respect to the Brown-Rho scenario for in-medium effects become visible only at invariant masses higher than 0.5 GeV, region where dileptons are mainly emitted by the decay of nucleonic resonances via intermediate vector meson propagation. For these two scenarios the discrepancies with experimental data are more evident as not even the slope of emission rate as a function of invariant mass does not match the data. The simulation including all contributions to in-medium self energies seem to come closer to experimental data as compared with the case when only resonant contributions are being considered. Discrepancies between theoretical predictions and experimental data when including only contributions from the Dalitz decay of π^0 and η mesons as well as nucleonic resonances have been reported by other groups as well and it has been suggested that the inclusion of contributions due to *pn* bremsstrahlung would alleviate the problem [29].

VI. FINAL CONCLUSIONS

We have presented an extension of the eVMD modl which allows the extraction of in-medium properties of pions and eta mesons, by including explicit couplings of these two mesons to resonances. Results for the in-medium spectral functions of π and η mesons resemble qualitatively those obtained by other groups, differences being due to mainly inclusion of a different set of possible decay channels and to a lesser extent to differences in the approaches.

Additionally, an effective model for the vacuum description of the ρ and ω vector mesons has been developed and making use of the eVMD and its extension just mentioned the in-medium corrections to the virtual pion cloud surrounding rho and omega vector mesons have been computed. As a general feature, if only contributions to due in-medium modifications of the pion cloud are considered an increase of mass of the vector mesons is obtained, more pronounced for the ω meson. A unified model which can be used to describe properties of both scalar (π and η) and vector mesons (ρ and ω) has thus been constructed allowing for the calculation of all contributions to the vector mesons self-energies at first order in an expansion over density.

Finally, a comparison of the theoretical dilepton spectrum with experimental data provided by the DLS and HADES

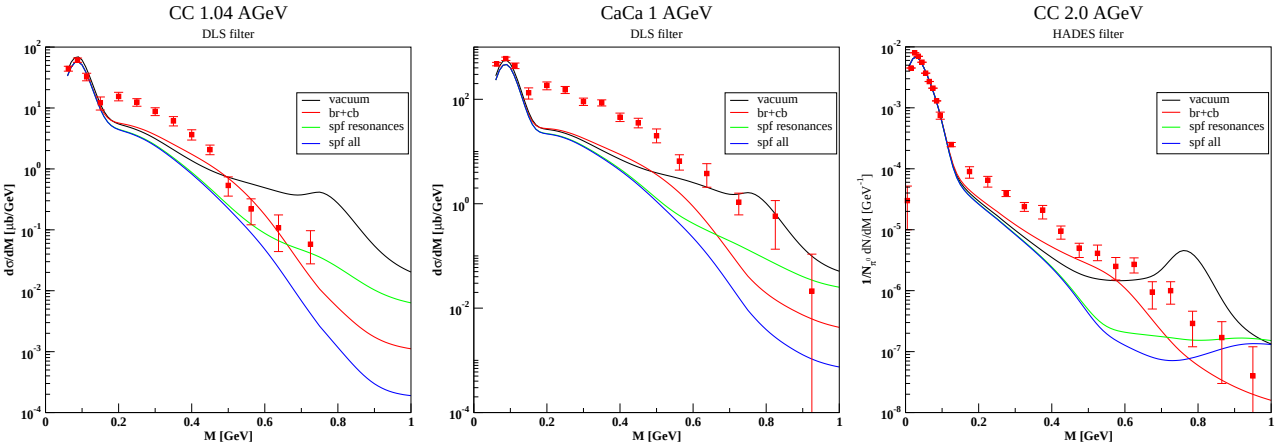

FIG. 8: Comparison between theoretical predictions of our model for dilepton emission rate in heavy-ion collisions with some of the experimental data. First two plots from left to right present a comparison of theoretical emission rates with the ones measured by the DLS collaboration for the C+C at 1.04 AGeV and respectively Ca+Ca at 1.04 AGeV. In the rightmost plot theoretical and experimental data for the reaction C+C at 2.0 AGeV measured by the HADES collaboration are compared.

collaboration reveals important difference for all in-medium effect scenarious considered. Furthermore a scenario which neglects in-medium influence on vector meson properties is clearly excluded by experimental data. Work in the direction of understanding the discrepancy between theoretical predictions and experimental data for the dilepton spectrum in heavy-ion collisions is in progress, complemented by an effort to further refine the resonance-meson effective model employed to describe in-medium properties of hadrons.

[1] G.E. Brown and M. Rho, Phys. Rev. Lett. **66**, 2720 (1991); Phys. Rep. **269**, 333 (1996).
[2] T. Hatsuda and S.H. Lee, Phys. Rev. C **46**, R34 (1992); S. Leuopold, *ibid.* **64**, 015202 (2001);
[3] C.M. Shakin and W.D. Sun, Phys. Rev. C **49**, 1185 (1994); M. Asakawa and C.M. Rho, Phys. Rev. C **48**, R526 (1993).
[4] M. Post, S. Leupold, and U. Mosel, Nucl. Phys. A **741**, 81 (2004).
[5] D. Cabrera, E. Oset, and M.J. Vicente Vacas, Nucl. Phys. A **705**, 90 (2002).
[6] F. Klingl, N. Kaiser, and W. Weise, Nucl. Phys. A **624**, 527 (1997).
[7] K. Saito, K. Tsushima, and A.W. Thomas, arXiv:nucl-th/98110311.
[8] M.F.M. Lutz, G. Wolf, and B. Friman, Nucl. Phys. A **706**, 431 (2002).
[9] P. Muehlich, V. Shklyar, S. Leupold, U. Mosel, and M. Post, Nucl. Phys. A**780**, 187 (2006).
[10] A. Faessler, C. Fuchs, and M.I. Krivoruchenko, Phys. Rev. C **61**, 035206 (2000).
[11] M.I. Krivoruchenko, B.V. Martemyanov, A. Faessler, and C. Fuchs, Ann. Phys. **296**, 299 (2002).
[12] A. Faessler, C. Fuchs, M.I. Krivoruchenko, and B.V. Martemianov, J. Phys. G **29**,603 (2003).
[13] E. Santini, M.D. Cozma, A. Faessler, C. Fuchs, M.I. Krivoruchenko, and B. Martemyanov, Phys. Rev. C **78**, 034910 (2008).
[14] R.J. Porter *et al.* [DLS Collaboration], Phys. Rev. Lett. 79, 1229 (1997).
[15] W.K. Wilson *et al.* [DLS Collaboration], Phys. Rev. **C57** (1998) 1865.
[16] G. Agachikiev *et al.* [HADES Collaboration], Phys. Rev. Lett. **98**, 052302 (2007).
[17] G. Agachikiev *et al.* [HADES Collaboration], Phys. Lett. B **663**, 43 (2008)
[18] M.D. Cozma "In-medium properties of vector mesons: nucleonic resonances effects"; Progress Report for the project "Hadron Properties in Nuclear Matter and Dilepton Emission in Relativistic Heavy-Ion Collisions", 15th Dec. 2007.
[19] S.J. Brodsky and G.R. Farrar, Phys. Rev. C **11**, 1309 (1975);
[20] K. Shekter, C. Fuchs, A. Faessler, M. Krivoruchenko, and B. Martemyanov, Phys. Rev. C **68**, 014904 (2003).
[21] V. Pascalutsa, and R. Timmermans, Phys. Rev. C **60**, 042201 (1999).
[22] R. Shyam, and O. Scholten, arXiv:nucl-th/0808.0632 (2008).
[23] T. Feuster, and U. Mosel, Phys. Rev. C **58**, 457 (1998).
[24] C. Fernandez-Ramirez, E. Moya de Geurra, and J.M. Udias, Ann. Phys. **32**, 1408 (2006)
[25] M. Urban, M. Buballa, R. Rapp, and J. Wambach, Nucl. Phys. A **641**, 433 (1998).
[26] C.L. Korpa and M.F.M. Lutz, Nucl. Phys. A **742**, 305 (2004).
[27] T. Inoue, and E. Oset, Nucl. Phys. A **710**, 354 (2002).
[28] K. Tsushima, D.H. Lu, A.W. Thomas, and K. Saito, Phys. Lett. B **443**, 738 (1991).
[29] E. Bratkovskaya, *Dileptons from heavy-ion collisions: from SIS to FAIR and off-shell transport*, talk given at the workshop "Electromagnetic probes for strongly interacting matter: the quest for medium modifications of hadrons", Trento, Italy

(2007).
[30] C. Fuchs, M.I. Krivoruchenko, H. Yadav, A. Faessler, B.V. Martemyanov, and K. Shekther, Phys. Rev. C **67**,025202 (2002).